Phosphatidylinositol 4,5-bisphosphate is an HCV NS5A Ligand and Mediates Replication of the Viral Genome

(Short title: PI(4,5)P2 mediates HCV replication)

Nam-Joon Cho[1,2*], Choongho Lee[1**], Phillip S. Pang[1,3***], Edward A. Pham[1,2], Benjamin Fram[1,2], Khanh Nguyen[1,2], Anming Xiong[1,2], Ella H. Sklan[1****], Menashe Elazar[1,2], Elif S. Koytak[1], Caroline Kersten[1], Kay K.Kanazawa [4], Curtis W. Frank[4], and Jeffrey S. Glenn[1,2,5,+].

[1]Department of Medicine, Division of Gastroenterology and Hepatology, Stanford University School of Medicine;

[2]Department of Microbiology and Immunology, Stanford University School of Medicine;

[3]Department of Medicine, Division of Infectious Diseases, Stanford University School of Medicine;

[4]Department of Chemical Engineering, Stanford University;

[5]Veterans Administration Medical Center, Palo Alto, California, United States of America.

* current address: Nanyang Technological University, Singapore
** current address: Dongguk University College of Pharmacy
*** current address: Gilead Sciences
**** current address: University of Tel-Aviv, Israel
+ To whom correspondence should be addressed:

Dr. Jeffrey S. Glenn, Department of Medicine, Division of Gastroenterology and Hepatology, Stanford University School of Medicine, Stanford University, CCSR

3115A, 269 Campus Drive, Stanford, CA, 94305-5187; Tel:(650) 725-3373; Fax:(650) 723-3032; Email: jeffrey.glenn@stanford.edu

Supplementary Methods and Materials.

Supplementary Fig. 1. Self-assembled biomimetic PI(4,5)P_2 containing polymerized, intact vesicle platform for the NS5A AH peptide binding studies.

Supplementary Fig. 2. Determination of K_d for the NS5A AH and PI(4,5)P_2 interaction.

Supplementary Fig. 3. Binding of full length NS5A to PI(4,5)P_2 and related phosphoinositides.

Supplementary Fig. 4. Mutation of the BAAPP domain does not alter the intracellular distribution of NS5A when expressed as an isolated protein.

Supplementary Fig. 5. Determination of k_{on} and k_{off} values for TBC1D20 binding to NS5A on membranes with or without PI(4,5)P_2 enrichment.

Supplementary Fig. 6. Binding of TBC1D20 protein to solid-supported human liver microsomal membranes in the absence of NS5A, with or without prior PI(4,5)P_2 enrichment.

Supplementary Fig. 7. An intact BAAPP domain is required for efficient replication of the HCV infectious clone.

Supplementary Fig. 8. Basic Amino Acid PI(4,5)P_2 Pincer (BAAPP) domains found in other AHs mediate specific binding of PI(4,5)P_2.

Supplementary Methods and Materials.

E4 Quartz Crystal Microbalance-Dissipation (E4 QCM-D)

Unlike conventional QCM-D models (e.g. Q-Sense D300), the Q-Sense E4 has a controlled flow system with four sensors that can be used in any serial or parallel configuration. The E4 system can measure the change of frequency and dissipation up to thirteen overtones. Adsorption kinetics and the viscoelastic properties of the adsorbed layer were studied using a Q-Sense E4 (Q-Sense AB, Gothenburg, Sweden) equipped with a parallel plate flow. AT-cut crystals (Q-Sense) of 14 mm in diameter with 50 nm thermally evaporated gold were used for all vesicle interaction and adsorption experiments. Each QCM crystal was treated with oxygen plasma at ~ 80 watts for ~ 5 minutes prior to measurements (March Plasmod Plasma Etcher, March Instruments, California, USA). For in situ measurements, one side of the QCM was sealed with a rubber o-ring. The crystal was initially driven near its resonance frequency as indicated by a maximum in the current. To capture the characteristic dissipation, the drive circuit was short-circuited and the exponential decay of the crystal oscillation was recorded and analyzed, yielding the frequency and dissipation changes at 5, 15, 25, 35, 45, 55, and 65 MHz. The typical sensitivity of the measurement in liquid is 1.77 ng/cm^2 corresponding to a 0.1 Hz frequency change and detectable change in energy dissipation in liquid is 0.1 x 10^{-6}. The temperature of the Q-Sense cell was set at 25.0°C and accurately controlled by a Peltier element in the cell with fluctuation smaller than ± 0.05°C.

Circular Dichroism (CD) Measurements

Circular dichroism (CD) measurements were carried out using an Aviv Model 215 equipped with a 450 watt Xenon arc lamp light source and a double-fused silica prism monochromator, range: 165-1200 nm MgF_2 polarizer. CD scans in wavelength mode were recorded in the range of 190 nm to 270 nm at 1.0 nm steps and averaged over two scans with averaging time = 5.0 sec/datum point. Measurements were carried out at 25°C with a thermoNeslab M25 recirculator and water bath. Spectral units were expressed as the molar ellipticity per residue by using peptide concentrations determined by measuring the UV light absorbance of tyrosine and tryptophan at 280 nm. The secondary scans were corrected for background based on blanks of PBS buffer.

Plasmids

Bart79I, a high-efficiency subgenomic replicon of HCV, harbors the neomycin resistance gene (neo) and the HCV nonstructural proteins. The Bart-Luciferase plasmid, Bart79I-luc, was cloned from the Bart79I parent and the pGL3-Basic parent (Promega), In brief, a NotI site was introduced after the 15th amino acid of Core in Bart79I using PCR mutagenesis. The luciferase gene was PCR amplified from the pGA3Basic plasmid using the primers NotLucS, GAATGCGGCCGCAATGGAAGACGCCAAAAACATAAAG, and LucDraAS, CGATTTAAATTACACGGCGATCTTTCCGCCC. The PCR product was ligated into the Bart79I plasmid following restriction digestions of both components with

NotI and DraI. Finally, the ScaI restriction site in the Luciferase coding region was removed by introducing a silent mutation in the site by PCR mutagenesis.

Purification of NS5A

NS5A from genotype 1b was cloned into pET28a carrying a C-terminal His-tag. His-tagged NS5A was purified as described (22) with minor changes. Briefly pET28a-NS5A was transformed into BL21(DE3) cells (Stratagene). Transformed cells were grown overnight in 25 mL Luria-Bertani (LB) media supplemented with kanamycin at 37° C. The overnight culture (diluted 1:100) was used to inoculate 1 L of kanamycin supplemented LB. The cells were grown at 37° C to an absorbance of 1. Isopropyl-β-D-thiogalactopyranoside (IPTG, Invitrogen)) was added to a final concentration of 0.5 mM and the cells were grown for an additional 4 h at 20 °C. Cells were pelleted by centrifugation and resuspended in 25 ml of lysis buffer (100 mM Tris, pH 8.0, 200 mM NaCl, 10 mM 2-mercaptoethanol and Complete mini protease inhibitor tablets (Roche)). After 15 min of incubation on ice, cells were lysed by French press cycles at a pressure of 10,000 p.s.i. for 1 min, PMSF was added to a final concentration of 1 mM and NP-40 to 0.5%. The extract was clarified by centrifugation at 27,000 × g for 30 min at 4 °C. The supernatant was then passed through a 0.45-μm filter and loaded onto a 40-mL DE52-cellulose column connected to a 1-ml HisTrap nickel-nitrilotriacetic acid column (GE Healthcare). The columns were washed with 1 column volume of lysis buffer. The Ni–NTA–agarose column was further washed with 10 mL of the lysis buffer and then with 5 mL lysis buffer containing 5 mM imidazole (Sigma). NS5A-His was eluted with lysis buffer containing 0.5 M imidazole. Fractions (0.75 mL) were collected and analyzed for

purity by SDS–PAGE. The fractions containing the majority of the protein were pooled and dialyzed against 50 mM Hepes, pH 7.5, 1 mM DTT overnight. The samples was aliquoted and stored at 80 °C. Sample concentration was determined by both Bradford assay and SDS–PAGE analysis.

Colony Formation Assays

5 micrograms of in vitro-transcribed wild type and mutant Bart79I RNAs were mixed with 6 x 10^6 Huh7 cells in RNase-free PBS (Biowhittaker) and transferred into a 2 mm-diameter gap cuvette (BTX, San Diego, CA). Electroporation was performed using a BTX model 830 electroporator. The electroporation condition was as follows: 680 V, five periods of 99 ms at 500 ms intervals. The electroporated cells were diluted in 10 ml of cell culture medium. Cells were transferred to 10 cm tissue culture dishes at different dilutions. At 24 hr postelectroporation, cells were supplemented with untransfected feeder Huh7 cells to a final density of 10^6 cells/plate. Twenty-four hours later, the medium was supplemented with G418 to a final concentration of 750 mg/ml. This selection medium was replaced every three days for three weeks. Following selection, the plates were washed with PBS, incubated in 1 % crystal violet in 20 % ethanol for 5 min, and washed five times with H_2O for colony counting.

Viral Sequencing Analysis

TRIzol reagent (Gibco BRL) was used to extract total RNA from the pool containing the Huh7 cells that survived the colony formation assays following

electroporation with in vitro-transcribed wild type or mutant Bart79I RNAs, as described by the manufacturer. SuperScript III one-step RT-PCR platinum Tag HiFi kit (Invitrogen, Carlsbad, CA) was used to reverse transcribe HCV RNA into DNA first and then amplify the NS5A region with two primers (FW-SspI-NS5A, GGATACAATATTTAGCAGGCTTGTCCAC, and RV-MluI-NS5A, TGGTGTACGCGTTAATGGGGAATGTT) covering the entire NS5A sequence. Amplified PCR DNA fragments were purified using PCR purification kits from QIAGEN. Purified DNAs were sent to Sequetech Inc (Mountainview, CA) for sequencing analyses.

Transient Replication Assays

10 micrograms of in vitro-transcribed wild type or mutant Bart79I-luciferase RNAs were electroporated into Huh7 cells as described above. The electroporated cells were diluted in 40 ml of cell culture medium. 2 ml of cells were aliquoted in 6 well tissue culture plates. Firefly luciferase activities were measured at 8, 48, 96, and 144 hr post electroporation by using a firefly luciferase kit from Promega (Madison, WI).

For transient replication assays to study the effect of BAAPP domain mutations within the context of an HCV infectious clone, 10 μg of wild type or mutant *in vitro*-transcribed FL-J6/JFH-5'C19Rluc2AUbi RNAs [1] were electroporated into Huh7 cells as described above. The electroporated cells were diluted in 18 ml of cell culture medium. 1 ml of cells was aliquoted in 6 well tissue culture plates.

Renilla luciferase activities were measured at 8, 48, 96, and 144 hr post electroporation using a Renilla luciferase kit from Promega (Madison, WI).

siRNAs

ON-TARGETplus SMARTpool combinations of 4 siRNAs each against PI4KIIIalpha (L006776, target sequences - GCUAUGUGCGGGAGUAUAU, GAUCGAGCGUCUCAUCACA, GUGGCCAACUGGAGAUCUA, and GGAACGAGUGACCCGUCU) and PIP5KIalpha (L004780, target sequences- ACACAGUACUCAGUUGAUA, GCACAACGAGAGCCCUUAA, GUGGUUCCCUAUUCUAUGU and GUAAGACCCUGCAGCGUGA) were purchased from Dharmacon (GE Healthcare). A non-targeting control siRNA (Dharmacon, D001810) was used as negative control.

Treatments with siRNAs

Two hundred thousand Huh7.5 cells were plated in a 24 well plate and incubated over night. The next day, cells were transfected with 25nM siRNA using Lipofectamine 2000 (Invitrogen) according to the manufacturer's protocol. The cells were incubated for 4 hours at 37^{o}C and then transferred to a 6 well plate; five thousand cells were plated in a 96 well plate in order to determine the effect of siRNA knockdown on target gene levels by quantitative PCR (see below). After over-night incubation, the cells were transfected again with a mix of 25nM siRNA and 1 microgram of in-vitro transcribed RLuc-J6/JFH1 RNA. Four-hours post transfection, the media was replaced and the cells were incubated for 72 hours to test for HCV replication. Cells were lysed with the Renilla

Luciferase Assay buffer (Promega) according to the manufacturer's protocol and activity was measured using a TECAN M1000 luminometer.

RT-qPCR:

To determine the effect of siRNA knock down on target genes, cells in 96 wells plate were lysed using Trizol reagent (Invitrogen) and RNA was extracted according to the manufacturer's protocol. One microgram of RNA was used for cDNA synthesis using the iScript Advanced cDNA Synthesis Kit (BioRad). One fifth of the cDNA reaction was used as template for qPCR using the TaqMan gene expression assay from Applied Biosystmes (PI4KIIIa- Hs01021084, PIP5KIa- Hs00801004) in a CFX96 Real Time PCR thermocycler (BioRad). Gene levels were normalized to GAPDH transcript and S18 RNA and expression level of the gene of interest was determined relative to non-targeting siRNA treated cells.

Cell lines with stably transduced shRNAs

Short hairpin RNAs (shRNAs) targeting PI4KIIIalpha (NM_002650.2, PIK4CA-1 , CCGGGGCTATGTGCGGGAGTATATTCTCGAGAATATACTCCCGCACATAGCCT TTTTG- TRCN0000219839 and PIK4CA-2, CCGGACGACATGATCCAGTACTATC CTCGAGGATAGTACTGGATCATGTCGTTTTTTG- TRCN0000219840) and PIP5KIalpha (NM_003557, PIP5K1A-3, CCGGATAGGCCATAGAAGTGTTGATCTCGAGATCAACA CTTCTATGGCCTATTTTTT- TRCN0000010142 and PIP5K1A-5, CCGGAGCCCT

GGTACATGACGGAGACTCGAGTCTCCGTCATGTACCAGGGCTTTTTT-TRCN0000010129) were from Sigma. Non-targeting shRNA from Sigma (SHC016-1EA) was used as negative control. Lentiviral particles were produced as previously described [2]. To establish stable gene knockdown cell lines, Huh7.5 cells were transduced with shRNA-encoding lentiviral particles. After 3 days, cells were split and selected with 4 μg/ml of puromycin (Sigma) for three weeks. The effect of shRNA knock down on target gene mRNA expression, was determined similarly to siRNA-treated cells, as described above.

shRNA experiments

To evaluate the effect of stable PI-kinase gene knockdown on HCV replication, 20,000 cells harboring an individual stably transduced shRNA (see above) were plated in each well of a 96-well plate under 2 μg/ml puromycin overnight. Cells were infected with Gaussia luciferase reporter HCV viral particles on the next day. After three days of infection, luciferase activity was measured. Alamar Blue in each well was also measured to account for cell viability.

Western blots:

Five hundred thousand Huh7.5 cells were transfected in a 6 well plate with 25nM siRNA using Lipofectamine 2000 and 24 hours after the first transfection, cells were transfected again with siRNA . The cells were transferred to a 10cc dish 4 hours post transfection and incubated for 72 hours. For shRNA expressing cells, 1.5 million cells were plated in a 10cc culture plate and grown for 72 hours. Proteins from the siRNA

transfected cells, or stably expressing shRNA cells, were extracted using the Total Protein Extraction kit (101Bio) and protein concentration was determined using the Bradford protein determination kit (BioRad). The cell lysate was supplemented with Laemmli sample buffer containing reducing agent followed by boiling for 5 minutes. Eighty micrograms of total protein were resolved on a 5.5% (PI4KIIIalpha) or 8% (PIP5KIalpha) SDS-PAGE and transferred to a PVDF membrane. Western blot was carried out using rabbit antibody against PI4KIIIalpha (Sigma-Aldrich, SAB2700958), rabbit antibody against PIP5KIalpha (ab137441, Abcam), or mouse antibody against beta actin followed by a HRP conjugated secondary antibody and detection using ECL reaction. Western blot films were scanned and bands of interest were quantified using Image J software. For loading control of PI4KIIIa westerns, the membrane was stained with Ponceau S stain.

Immunofluorescence Microscopy

Coverslips were stained with rinsed in phosphate-buffered saline (PBS) three times. They were fixed at room temperature for 15 min in 4 % paraformaldehyde, permeabilized in 0.1 % Triton-X in PBS for 5 min, rinsed three times in PBS, and blocked with PBS containing 2 % fetal bovine serum (FBS). Anti-PI(4,5)P_2 (1:300, 2C11, Echelon Bioscience Inc., Salt Lake City, UT) or anti-NS5A (1:1000, 6F3, Virostat, Portland, ME) antibodies were applied, and the mixture was incubated for 2 hr. After three washes in PBS, coverslips were incubated with Alexa 594-conjugated anti-mouse IgM secondary antibody for PI(4,5)P_2 or Alexa 488-

conjugated anti-mouse IgG secondary antibody for NS5A (Invitrogen, Carlsbad, CA) for 1 hr. Following three washes with PBS, coverslips were mounted onto slides using Prolong Gold anti-fade reagent with DAPI (Invitrogen, Carlsbad, CA) and sealed. Fluorescent signals were examined and captured by LSM 510 Carl Zeiss confocal laser scanning microscope.

Supplementary Fig. 1 Self-assembled biomimetic PI(4,5)P_2-containing polymerized, intact vesicle platform for the NS5A AH peptide binding studies

In order to study the specific interaction between the NS5A AH and PI(4,5)P_2, we created the stable platform as shown in Supplementary Fig. 1. There are two main reasons to utilize polymerized, intact vesicles as a sensitive sensor platform. First, it has been well-demonstrated that PI(4,5)P_2 has a net charge depending on surrounding environmental factors such as local pH and its molecular interactions [3]. It is known that the net valence charge may be as high as -4 acting as a concentrated electrostatic site [3]. Therefore, utilizing a supported bilayer platform as a sensor has stability issues because of the dewetting behavior of PI(4,5)P_2 molecules due to repulsion from the hydroxyl groups of the SiO_x substrate. Furthermore, even though we created complete bilayers, there often remained intact or adsorbed vesicles that hindered detection of PI(4,5)P_2-AH peptide binding due to rupture of the vesicles by AH peptides (during the rupturing process, there is a loss of mass and increase in frequency associated with the vesicle to bilayer transformation [4]. Secondly, in the course of our previous studies regarding AH peptide interaction with vesicles, we found and reported that the AH peptide has vesicle lysis potential [4]. In order to prevent this, we polymerized the vesicles using polydiacetylene photochemistry. The resulting platforms have superior detection dynamic range (c.f. surface area, stability, and robustness). Briefly, PI(4,5)P_2-containing vesicles contain a covalent, conjugated

ene-yne network in the acyl chains that was catalyzed by UV irradiation as shown in Supplementary Fig. 1a. Further, in order to ensure a uniform size distribution of the polymerized vesicles, we employed the extrusion method (400 nm track-etched polycarbonate membrane) followed by bath sonication, resulting in polymerized vesicles with an average size of 198 ± 6.7 nm and a polydispersity of 0.23 ± 0.02, respectively. The zeta potential (ζ) of obtained $PI(4,5)P_2$-containing polymerized vesicles is ~ -19 mV ± 2.3 mV (PC-diyne, PE-diyne, and PIPs –diyne; 65:30:5 molar ratio), well within range of previous research [3,5]. The resulting $PI(4,5)P_2$-containing vesicles are coated on the SiO_x quartz crystal as shown in Supplementary Fig. 1b. Similar vesicle platforms were also prepared with other PIPs. As we anticipated, unlike conventional vesicle adsorption kinetics (that display a characteristic vesicle rupturing signature [6]), the polymerized vesicles do not rupture, but instead display typical intact vesicle adsorption kinetics, indicating a stable sensor platform [6,7]. Of note, the various intact PI-containing vesicle platforms had slightly different masses due to intrinsic factors such as lipid composition and zeta potential. Nonetheless, the physical properties of the platforms (i.e., intact vesicle adlayer with similar membrane curvature and viscoelasticity) were preserved. In order to correct for these minor mass deviations, we normalized the binding mass values based on the minor deviations of the initial platform masses. The binding mass of peptide was calculated using the Sauerbrey model, which relates the change in resonance frequency to the change in adsorbed mass. Although this relationship is not fully valid to describe binding upon the viscoelastic, intact vesicles, it can be utilized in

this case where peptide binding is either so significant or minor that slight deviations due to this error in actual mass are insignificant for the results and conclusions of the QCM-D assay. The picture illustrates PI(4,5)P_2-containing intact polymerized vesicles on the SiO_x substrate (Supplementary Fig. 1c)

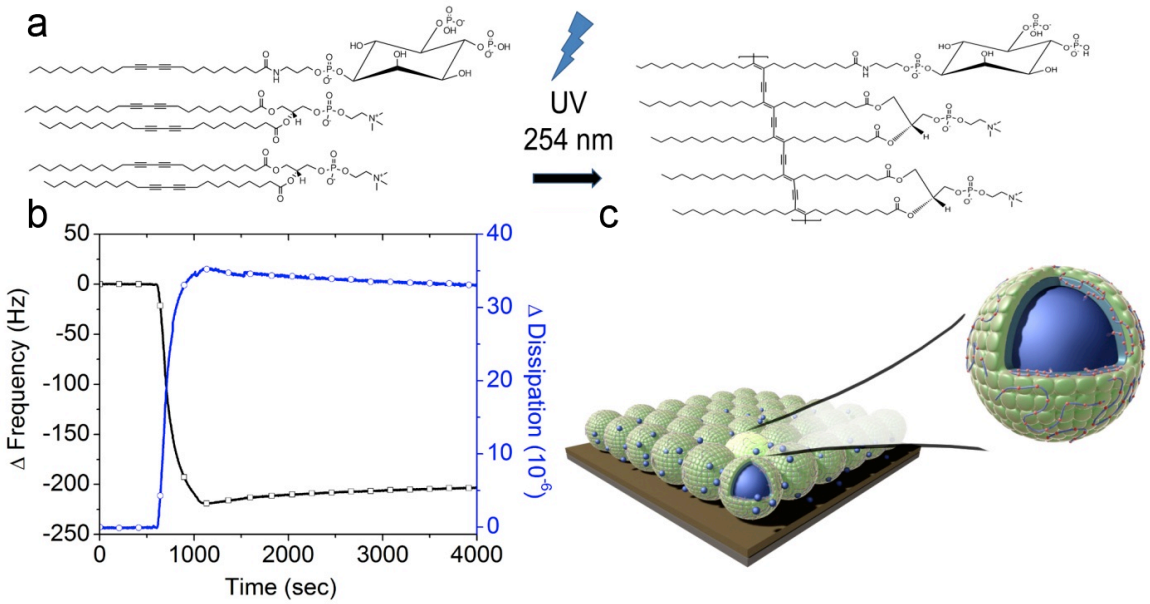

Supplementary Fig. 1. Self-assembled biomimetic PI(4,5)P_2-containing polymerized, intact vesicle platform for the NS5A AH peptide binding studies

(a) Schematic representation of the covalent, conjugated ene-yne network in the acyl chains upon UV irradiation. **(b)** The typical QCM kinetics for creation of the intact vesicle platform on a SiO_x substrate. **(c)** An illustration of PI(4,5)P_2-containing polymerized, intact vesicles as a sensor platform. Blue balls represent water molecules.

Supplementary Fig. 2 Determination of K_d for the NS5A AH and PI(4,5)P_2 interaction

The average K_d was determined by curve fitting to one-site binding using Prism 4.0 software (GraphPad Software Inc., San Diego, CA) yielding an average binding constant of 4.5 μM for the NS5A AH peptide binding on the PI(4,5)P_2-containing polymerized vesicle platform. Alternately, one can also use the modified Langmuir isotherm to fit the curve, which gives us similar results.

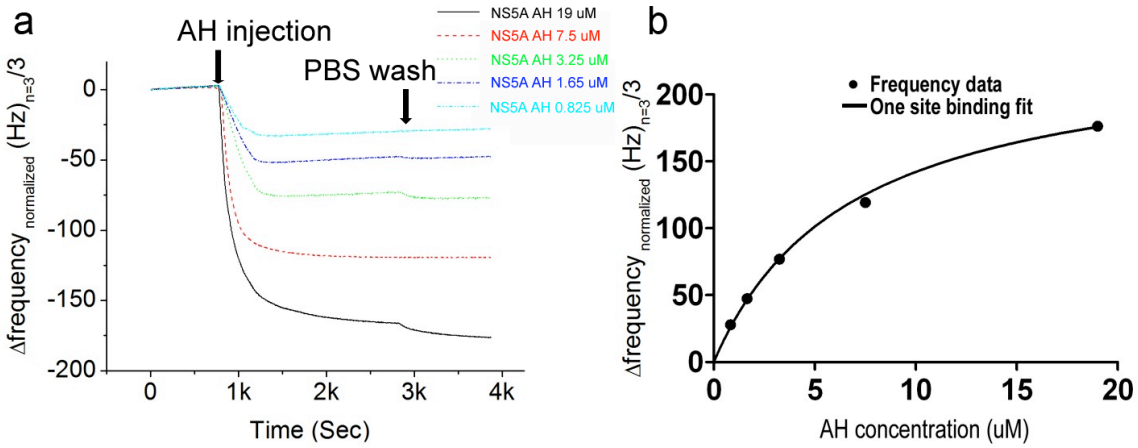

Supplementary Fig. 2. (a) Concentration dependence of the NS5A AH peptide binding on intact PI(4,5)P_2-containing vesicle platform and (b) use of a one-site binding kinetic model in order to calculate the K_d of the NS5A AH peptide binding to PI(4,5)P_2

Supplementary Fig. 3. Binding of full length NS5A to PI(4,5)P_2 and related phosphoinositides.

To provide additional evidence supporting the specific binding of the NS5A AH to PI(4,5)P_2, and to confirm that the results obtained with the isolated NS5A AH peptide appropriately reflect the behavior of this AH segment when present in the context of the full length NS5A protein, we assessed the binding of full length NS5A protein to PI(4,5)P_2 and related phosphoinositides (PI(3,4)P_2 and PI(3,5)P_2,) using the method of Fig. 1a. Similar to the latter, the purified full length NS5A protein (Coomassie stain, left panel) exhibits substantial binding to PI(4,5)P_2 , and preferential binding to PI(4,5)P_2 over the other PI-bisphosphate isoforms was observed (right panel).

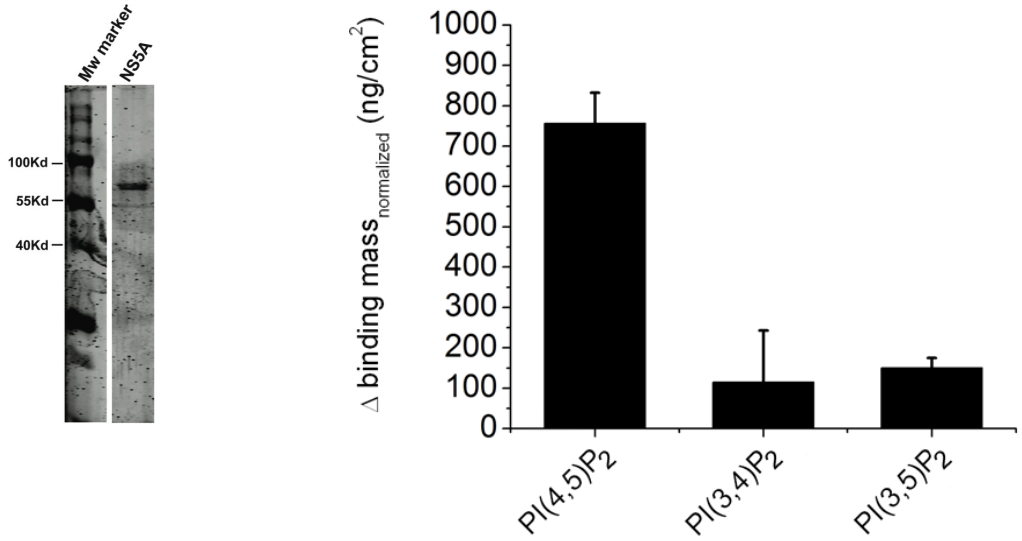

Supplementary Fig. 4. Mutation of the BAAPP domain does not alter the intracellular distribution of NS5A when expressed as an isolated protein.

(A) Plasmids encoding wild-type NS5A fused to eGFP, and NS5A with BAAPP domain mutations K20A&K26A fused to DsRed, were co-transfected into Huh7 cells, followed by fluorescent microscopy. **(B)** In contrast, when NS5A (tagged with YFP) is expressed in the context of a replicating HCV replicon (as in Fig. 3B), all the NS5A co-localizes with cytoplasmic PI(4,5)P_2 speckles. To confirm that the remaining substantial proportion of PI(4,5)P_2 is indeed localized in the nucleus, DAPI staining was performed. Scale bar = 5μM. Magnification 100X.

(A)

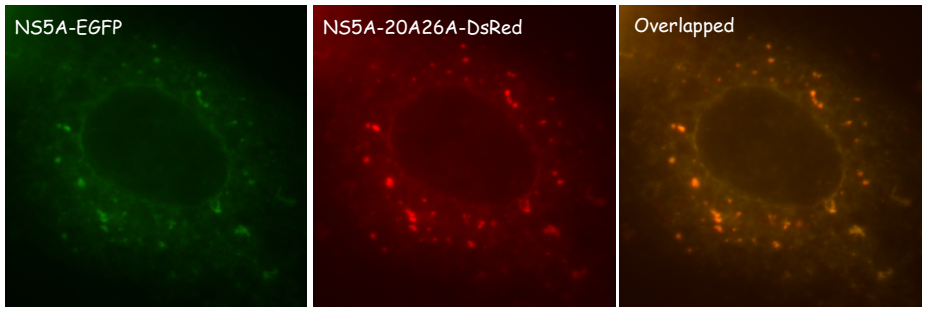

(B)

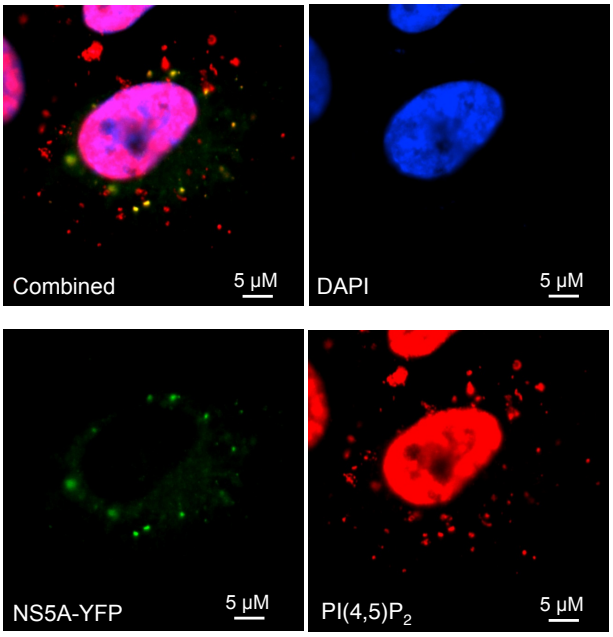

Supplementary Fig. 5. Determination of k_{on} and k_{off} values for TBC1D20 binding to NS5A on membranes with or without PI(4,5)P_2 enrichment.

We utilized a novel "membrane-on-a-chip" system—previously developed by our group for binding kinetic measurements of protein-protein interactions [8]—to detect binding of NS5A full-length protein to human liver microsomal membranes. To do so, human liver membranes were assembled as a sensor platform in order to detect the binding of foreign molecules (in this case, TBC1D20) using the quartz crystal microbalance with dissipation monitoring (QCM-D). QCM-D allows for measuring nanogram mass changes based on changes in frequency (Δf), and energy dissipation (ΔD) that occur when membranes or proteins bind to an oscillating SiO_x-coated quartz crystal [8]. As described and experimentally verified by the Sauerbrey [9] or Voigt-based models [8,10], the frequency change is a direct function of the mass change, where the frequency decreases with increased bound mass. Energy dissipation changes (ΔD) can be measured if the adsorbed film (i.e. bound membrane) is viscoelastic. Three different human liver membrane platforms were utilized: human liver membrane microsome with no additional PIP_2, or human liver membrane enriched with either PI(3,5)P_2 or PI(4,5)P_2 by vortexing. The resulting platforms demonstrated similar frequency and dissipation signatures and provided a stable, reproducible system to study protein-protein interactions (data not shown). In order to calculate kinetic constants of adsorption (k_{on}) and desorption (k_{off}) of TBC1D20 to NS5A, we utilized a modified Langmuir adsorption isotherm model. Modification of the

simple Langmuir isotherm model was made necessary by the lack of full reversibility of the adsorbed species during desorption, as evident in Figure 4b of the main report. We modified the adsorption process to include a two-site binding process, which included the usual reversible Langmuirian adsorption sites plus independent sites where the adsorption is irreversible. The reversible Langmuirian sites are characterized by k_{on} and k_{off}. The irreversible sites are characterized by a deposition rate constant, k_{ir}. We calculated k_{ir} and $K_{binding}(k_{on}/k_{0ff})$ using the following method. First, k_{off} was calculated by studying the desorption curve. Using the value of k_{off} fitted from the desorption curve, we then fitted a two-site adsorption to determine the value for the k_{on} and k_{ir}. Our interest, of course, centers on k_{on} and k_{off}, which we used to calculate $K_{binding}$. The equation describing the adsorption kinetics (Langmuir) is:

$$\frac{dn_R}{dt} = k_{on}(N_R - n_R)C - k_{off}n_R \qquad (1)$$

where n_R is the areal density of adsorbed species, N_R is the total number of reversible Langmurian sites and C is the concentration of TBC1D20, Since the relation between the areal density and the frequency change is related by a fixed constant, equation (1) also describes the frequency change, with the n's and N replaced by the change in frequency Δf. However, for pedagogical reasons, we continue the analysis in terms of the areal densities. The initial condition for n_R during the adsorption process is taken to be zero. In the case of desorption, we assume that the concentration is zero and equation (1) simplifies to:

$$\frac{dn_R}{dt} = -k_{off} n_R \qquad (2)$$

where n_R now denotes the desorbing species and is taken to have an initial value n_R^{INIT}.

Case of Desorption:

The solution to equation (2) can be written as follows:

$$n_R = n_R^{INIT}(1 - e^{-k_{off} t}) \qquad (3)$$

The fit to the desorption curves for the cases of No PIP and $PI(3,5)P_2$ are shown in Supplementary Fig. 5 A and B. In Supplementary Fig. 5C, where we have assumed no desorption, the calculated value is a constant. The experimental data were fitted to equation (3) to obtain values for n_R^{INIT} and k_{off}.

Case of Adsorption:

While the process of adsorption for the reversible Langmurian sites was given by equation (1), we must also consider the possibility of adsorption to the irreversible sites.

The following equation was employed to describe this two-site binding model:

$$n(t) = N_R \frac{k_{on} C}{k_{on} C + k_{off}} (1 - e^{-(k_{on} C + k_{off})t}) + n_{IR}^{INIT}(1 - e^{-(k_{IR} C)t}) \qquad (4)$$

In equation (4), the first term is the solution to equation (1) and describes adsorption to the reversible Langmurian sites while the second term describes

adsorption to the irreversible sites. Note that N_R is the total number of reversible sites and n_R^{INIT} is the total number of irreversible sites. Using equation (4), we varied N_R, k_{on}, and k_{ir} to fit the adsorption data. The quality of the fit provided a clue regarding the applicability of this two-site model.

The comparison to the experimental data is shown in Supplementary Fig. 5. The experimental data are shown by the light gray line and the calculated fit is shown by the dark dashed line. The fits for No PIP_2 and PI(3,5)P2 are in good agreement. For the case of PI(4,5)P_2, we fitted the adsorption to a simple Langmurian, assuming that k_{off} was zero. The values for the various parameters are shown in Supplementary Fig. 5G. Note that the value related to desorption in the case of PI(4,5)P_2 has been labeled "N/A", i.e. not applicable because the desorption curve could not be analyzed for that case (Supplementary Fig. 5C).

Supplementary Fig. 5. Langmuir isotherm fit to determine k_{on} and k_{off} values for TBC1D20 binding to NS5A on membranes with or without $PI(4,5)P_2$ enrichment.

For the two curves (**(A)** No PIP_2 and **(B)** $PI(3,5)P_2$), we obtained the maximum frequency value, k_{on}, k_{off}, and the apparent binding constant $K_{binding}$. For **(C)**, however, knowing that part of the adsorption on PI(4,5,P2) was irreversible, we cannot fit with standard Langmuir isotherm adsorption model. We only can fix the value for the dissociation rate constant and fit the initial adsorption curve to this two-site model for **(D)** No PIP_2 , **(E)** $PI(3,5)P_2$, and **(F)** $PI(4,5)P_2$. **(G)** The table summarizes the fitting values for adsorption and desorption of the TBC1D20 on NS5A for the indicated membrane platforms.

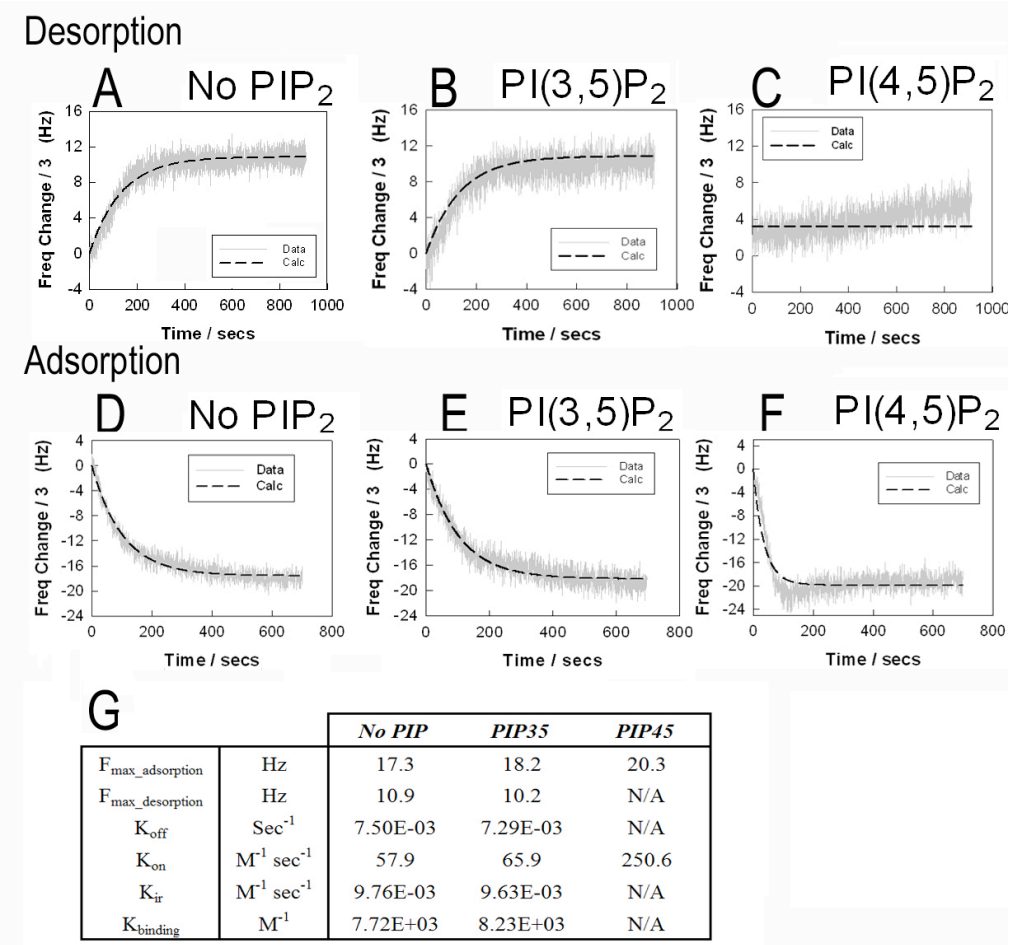

G

		No PIP	*PIP35*	*PIP45*
$F_{max\_adsorption}$	Hz	17.3	18.2	20.3
$F_{max\_desorption}$	Hz	10.9	10.2	N/A
K_{off}	Sec^{-1}	7.50E-03	7.29E-03	N/A
K_{on}	M^{-1} sec^{-1}	57.9	65.9	250.6
K_{ir}	M^{-1} sec^{-1}	9.76E-03	9.63E-03	N/A
$K_{binding}$	M^{-1}	7.72E+03	8.23E+03	N/A

Supplementary Fig. 6. Binding of TBC1D20 protein to solid-supported human liver microsomal membranes in the absence of NS5A, with or without prior PI(4,5)P_2 enrichment. QCM-D monitoring was employed to track the adsorption of human liver microsomal membranes with (red) and without (black) prior PI(4,5)P_2 enrichment onto a silicon oxide substrate (arrow 1), followed by addition of TBC12D20 protein to the biomembrane platform (arrow 2). Changes in the QCM-D frequency **(A)** and energy dissipation **(B)** signals were monitored. The observed frequency changes upon addition of TBC12D20 to the respective membranes were converted to changes in bound mass **(C)** by use of the Sauerbrey equation, as in Figure 1 of the main manuscript. Note that there were no significant differences (Student's T test) in TBC1D20 binding to PI(4,5)P_2 enriched vs. unenriched membranes in the absence of prior NS5A addition.

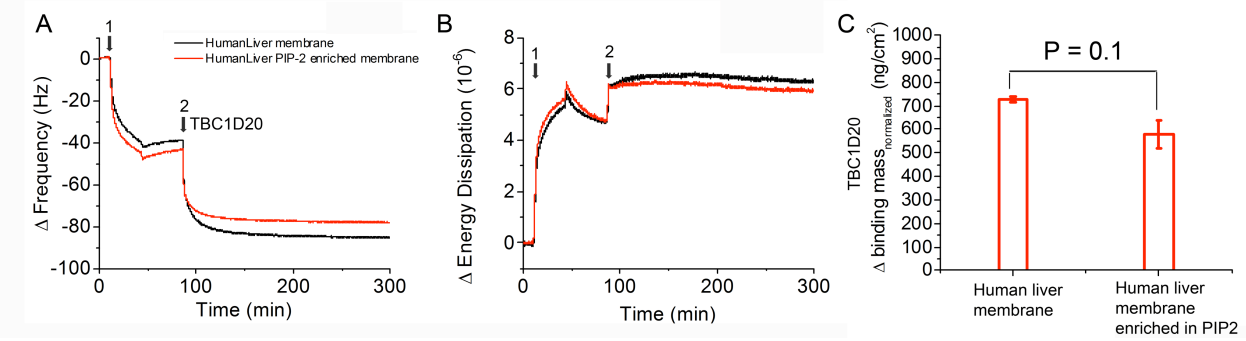

Supplementary Fig. 7. PI(4,5)P_2 mediates HCV RNA genome replication within the context of an HCV infectious clone. **(A)** Mutations (K20A alone, K26A alone, or the combination of K20A and K26A) were introduced into the NS5A BAAPP domain of a luciferase reporter-linked 2a infectious clone. Transient HCV replication assays were then performed as described in the Materials and Methods with individual mutant or wild-type clones. Replication efficiencies are expressed as a percentage of wild-type. We next validated the function and specificity of a collection of siRNAs against PI4KIIIalpha and PIP5Kalpha (panels B-G). **(B)** siRNAs against PI4KIIIalpha knock down their intended target mRNA. A collection of SmartPool siRNAs targeting PI4KIIIalpha (see methods for specific sequences of individual siRNAs within the SmartPool) (right column), or control non-targeting siRNA (left column), were transfected into Huh7.5 cells and the effect on the targeted PI4KIIIalpha mRNA was determined by qPCR. Values expressed relative to non-targeting control. T-test indicates significance. **(C)** siRNAs against PIP5Kalpha knock down their intended target mRNA. A collection of SmartPool siRNAs targeting PIP5Kalpha (see methods for specific sequences of individual siRNAs within the SmartPool) (right column), or control non-targeting siRNA (left column), were transfected into Huh7.5 cells and the effect on the targeted PIP5Kalpha mRNA was determined by qPCR. Values expressed relative to non-targeting control. T-test indicates significance**.** **(D)** siRNAs against PI4KIIIalpha are indeed specific for their intended target and do not affect the level of PIP5Kalpha mRNA. The SmartPool siRNAs targeting PI4KIIIalpha (right column), or control non-targeting siRNA (left column), were

transfected into Huh7.5 cells and the specificity for PI4KIIIalpha was demonstrated by observing a lack of off-target effect on the level of PIP5KIalpha mRNA, as determined by qPCR. **(E)** siRNAs against PIP5KIalpha are indeed specific for their intended target and do not affect the level of PI4KIIIalpha mRNA. The SmartPool siRNAs targeting PIP5KIalpha (right column), or control non-targeting siRNA (left column), were transfected into Huh7.5 cells and the specificity for PIP5KIalpha was demonstrated by observing a lack of off-target effect on the level of PI4KIIIalpha mRNA, as determined by qPCR. **(F)** Additional assessment of the efficacy and specificity of the above siRNAs. Western blot of Huh7.5 cells transfected with the above non-targeting, PI4KIIIalpha, or PIP5KIalpha siRNAs, respectively, probed with anti-PI4KIIIalpha antibody (top panel). Quantitation of the PI4KIIIalpha signal relative to the non-targeting control is indicated below the blot. Bottom panel: loading control provided by Ponceau S staining of the total proteins present on the blot. **(G)** Additional assessment of the efficacy and specificity of the above siRNAs. Western blot of Huh7.5 cells transfected with the above non-targeting, PIP5KIalpha, or PI4KIIIalpha siRNAs, respectively, probed with anti- PIP5KIalpha antibody (top panel). Quantitation of the PIP5KIalpha signal relative to the non-targeting control is indicated below the blot. Bottom panel: loading control provided by probing the blot with antibody to beta actin. **(H)** Transient HCV replication assays performed as in panel (A) above after prior transfection of the above non-targeting, PI4KIIIalpha, or PIP5KIalpha SmartPool siRNAs. Replication efficiencies are expressed as a percentage of non-targeting control. T-tests

indicate significance. To provide additional evidence in support of the above results obtained with siRNAs, we performed similar experiments with cell lines transduced to stably express individual shRNAs: two designed against PI4KIIIalpha ("shRNA-4α1" and "shRNA-4α2") and two designed against PIP5KIalpha ("shRNA-5α5" and "shRNA-5α3"). **(I)** Huh7.5 derived cell lines transduced to stably express either a control non-targeting shRNA (left), or one of two different shRNAs against PI4KIIIalpha (middle and right) were analyzed by Western blot probed with anti-PI4KIIIalpha antibody (top panel) to determine the effect of the shRNAs on the targeted PI4KIIIalpha. Quantitation of the PI4KIIIalpha signal relative to the non-targeting control is indicated below the blot. Bottom panel: loading control provided by Ponceau S staining of the total proteins present on the blot. **(J).** Huh7.5 derived cell lines transduced to stably express either a control non-targeting shRNA (left), or one of two different shRNAs against PIP5KIalpha (middle and right) were analyzed by Western blot probed with anti- PIP5KIalpha antibody (top panel) to determine the effect of the shRNAs on the targeted PIP5KIalpha. Quantitation of the PIP5KIalpha signal relative to the non-targeting control is indicated below the blot. Bottom panel: loading control provided by probing the blot with antibody to beta actin.

Next, the effect of the above shRNAs on HCV replication was assessed (panels K and L). **(K)** Transient HCV replication assays performed as in panel (A) using the cell lines of (I) that stably express the indicated non-targeting or anti-PI4KIIIalpha shRNAs. Replication efficiencies are expressed as a percentage of non-targeting control. T-tests indicate significance. **(L)** Transient HCV replication

assays performed as in panel (A) using the cell lines of (J) that stably express the indicated non-targeting or anti-PIP5KIalpha shRNAs. Replication efficiencies are expressed as a percentage of non-targeting control. T-tests indicate significance**.**

Note, the shRNA determined to have no effect on PIP5KIalpha in (J) above (shRNA-5α3) has no effect on HCV replication. T-tests indicate significance**.**

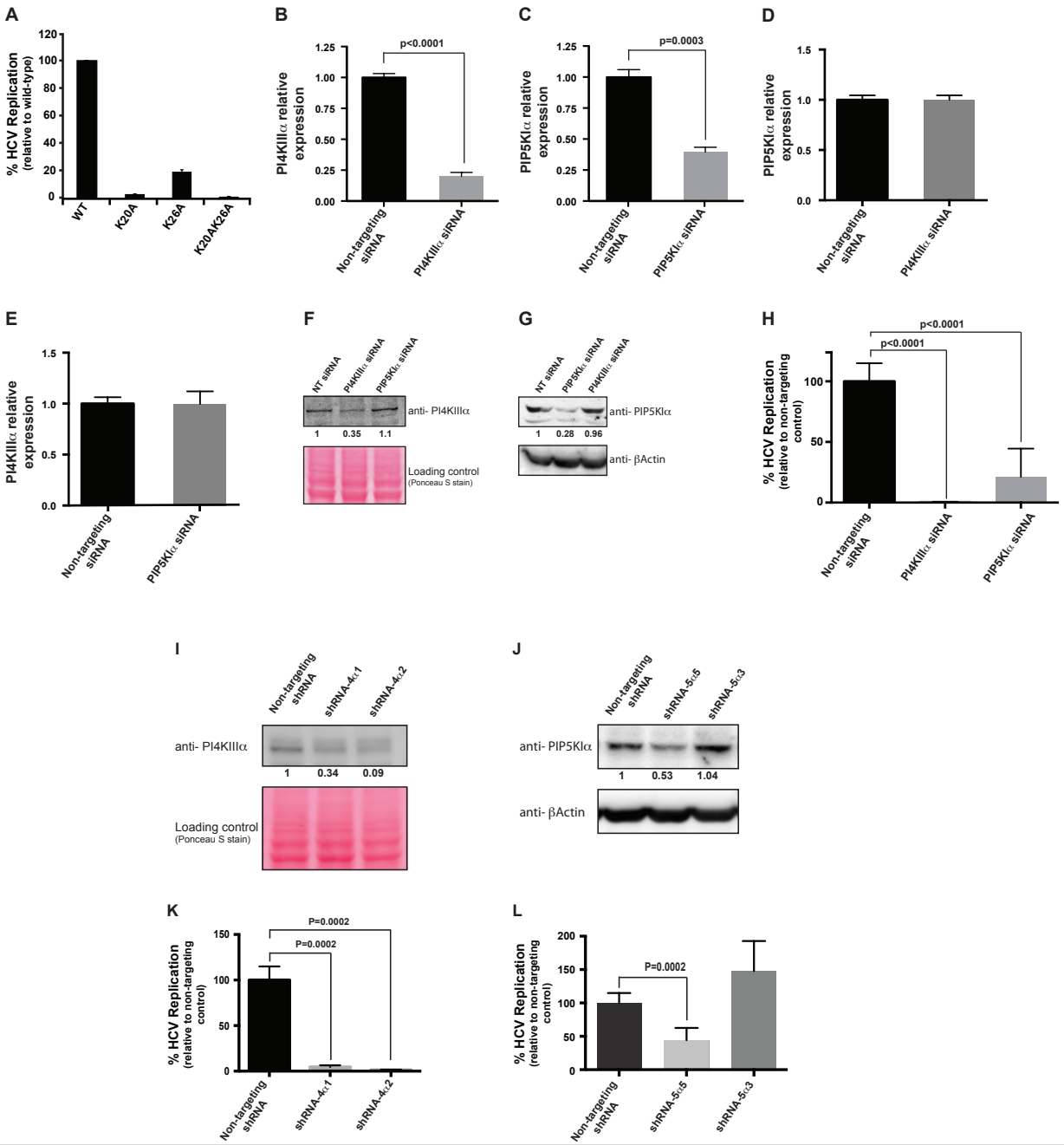

Supplementary Fig. 8. Basic Amino Acid PI(4,5)P_2 Pincer (BAAPP) domains found in other AHs mediate specific binding of PI(4,5)P_2.

QCM-D measurements, quantifying mass changes due to the binding of AH peptides harboring BAAPP domains from the indicated proteins of Figure 6 (main text) to vesicles containing either PI(4,5)P_2, PI(3,4)P_2, or PI(3,5)P_2 . **(A)** Apo B, **(B)** Enterovirus 2C, **(C)** JEV core, **(D)** HCV NS4B, and **(E)** Rhinovirus 2C. Methods were as in Figures 1 and 2 of the main text.

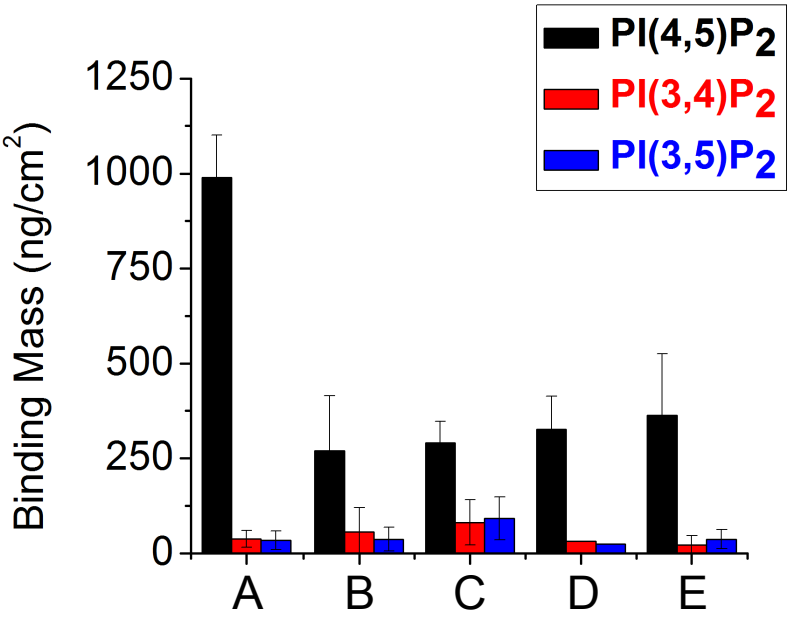

Supplementary Information References

1 Tscherne, D. M. *et al.* Time- and temperature-dependent activation of hepatitis C virus for low-pH-triggered entry. *J Virol* **80**, 1734-1741 (2006).

2 Xiong, A. *et al.* Isolation of human fetal liver progenitors and their enhanced proliferation by 3-D co-culture with endothelial cells. *Tissue Eng* **14**, 995-1006 (2008).

3 McLaughlin, S. & Murray, D. Plasma membrane phosphoinositide organization by protein electrostatics. *Nature* **438**, 605-611, doi:10.1038/nature04398 (2005).

4 Cho, N. J., Cho, S. J., Cheong, K. H., Glenn, J. S. & Frank, C. W. Employing an amphipathic viral peptide to create a lipid bilayer on Au and TiO2. *J Am Chem Soc* **129**, 10050-10051 (2007).

5 Ferguson, C. G. *et al.* Phosphoinositide-containing polymerized liposomes: stable membrane-mimetic vesicles for protein-lipid binding analysis. *Bioconjug Chem* **16**, 1475-1483 (2005).

6 Keller, C. A. & Kasemo, B. Surface specific kinetics of lipid vesicle adsorption measured with a quartz crystal microbalance. *Biophys J* **75**, 1397-1402, doi:10.1016/s0006-3495(98)74057-3 (1998).

7 Cho, N. J., Kanazawa, K. K., Glenn, J. S. & Frank, C. W. Employing two different quartz crystal microbalance models to study changes in viscoelastic behavior upon transformation of lipid vesicles to a bilayer on a gold surface. *Anal Chem* **79**, 7027-7035 (2007).

8 Cho, N.-J., Cheong, K. H., Lee, C., Frank, C. W. & Glenn, J. S. Binding dynamics of hepatitis C virus' NS5A amphipathic peptide to cell and model membranes. *J. Virol.* **81**, 6682-6689 (2007).

9 Sauerbrey, G. Verwendung von Schwingquarzen zur Waegun duenner Schichten und zur Mikrowaegung. *Z. Physik* **155**, 206 (1959).

10 Voinova, M. V., Rodahl, M., Jonson, M. & Kasemo, B. Viscoelastic acoustic response of layered polymer films at fluid-solid interfaces: Continuum mechanics approach. . *Phys Scripta.* **59**, 391-396 (1999).